Z. Zeren, et al., Int. J. Comp. Meth. and Exp. Meas., Vol. 5, No. 1 (2017) 66–75

OPTIMIZATION OF ELECTRON BEAM GENERATED INCLINED CONICAL PIN FINS FOR EFFICIENT HEAT SINKS

Z. ZEREN[1], K. HILLEWAERT[1], T. PINTO[2], A. FERHATI[2], M. SERRI[3] & M. MALAGUTTI[3]
[1]Cenaero, 29, Rue des frères Wright, Gosselies, Belgium.
[2]TWI Ltd, Granta Park, Great Abington, Cambridge, CB21 6AL, U.K.
[3]COOLTECH S.r.l., Via Camillo Prampolini, 30, 41043 Formigine, Italy.

ABSTRACT

This study reports the results of a numerical investigation and optimization of the hydrodynamic and thermal performance of two new types of pin-fin and plate-fin heat sinks. The first type consists of inclined cones and is inspired by the larger heat transfer extents in impinging flow conditions, whilst the second type concerns wavy form plate-fins chosen such as to combine the effects of thermal boundary layer re-initialization, flow separation and large heat transfer area of classical plate fins. Fairly complex features are considered, which cannot be manufactured easily using traditional approaches. However, in this study we exploit the manufacturing flexibility offered by a new surface-structuring technology, which allows to produce more complex geometries than possible with the current state-of-the-art techniques. A simplified numerical methodology has been proposed to decrease the computational cost, which was then validated with respect to the literature and the laboratory tests. Baseline versions of the two proposed geometries were compared to more common geometries found in the literature in order to make a first choice. The results show that the inclined cone features can increase the heat transfer coefficient, especially in inverse configuration, whereas the wave structures require very large pressure losses to achieve similar levels of thermal performance. Subsequently, only inclined cones have been optimized using an Evolutionary Algorithm optimization platform. The optimized geometries increase the overall performance, especially reducing the pressure drop, in comparison to the geometries found in the literature.

Keywords: heat sink, inclined cone, surfi-sculpt® process, wave structures.

1 INTRODUCTION

The rapid increase in the number of transistors per unit area in microelectronic devices leads to high heat loads. As a consequence, compact and efficient thermal management systems are required. Heat sinks transfer the generated heat from the electronic device to the working fluid or coolant due to direct contact. Heat generated from the electronic device is conducted through the heat sink material to the surface of contact and is then transferred to the coolant. Then the transferred heat is transported away by the fluid put into motion by natural or forced convection. The efficiency of the heat sink is determined by: (a) the wetted area, (b) the flow pattern induced by the geometry and arrangement, and (c) the fluid properties and the flow regime. In addition to maximizing the wet area, the flow pattern should be designed such that the build up of large thermal boundary layers on the solid surface is avoided, whilst flow impingement and mixing is enhanced. However, these design criteria, meant to increase the hlleat transfer efficiency, conflict with the requirement to limit the pumping power, which is impacted by the increased friction-related losses on the increased surface and the mixing losses due to complex flow patterns. Thus, finding an efficient heat sink surface is to balance between high heat transfer rate and low frictional losses.

The compromise between the conflicting design objectives is difficult and leads the industry to the use of, among others, pin-fin heat sinks, which, research shows to have enhanced

© TWI Ltd 2016
ISSN: 2046-0546 (paper format), ISSN: 2046-0554 (online), http://www.witpress.com/journals
DOI: 10.2495/CMEM-V5-N1-66-75

heat transfer with only moderate increase in pressure loss. Despite the volume of literature on the subject, there still does not appear to be a consensus about the most efficient pin shape. Literature includes a large number of studies that compare the pin-fin geometries, such as ellipse, cylinder and square as well the arrangements such as staggered or in-line. Using the well-known Entropy Generation Minimization method, Khan *et al*. [1] showed that for relatively low Reynolds numbers (<1000, based on the hydraulic diameter of pin cross-section and the uniform approach velocity), the ellipse shape provides the best performance. Jonsson and Bjorn [2] recommend elliptical pin-fins at high velocities and the circular pins at mid-range velocities. Concerning the flow direction, as argued by Duan and Muzychka [3], the impinging flow is expected to give higher thermal efficiency than the cross-flow application. Lee *et al*. [4] also consider thermal boundary layer re-initialization through the subdivision of the flow inside the pin array. In this case, the interruption of the fluid path increases the heat transfer efficiency considerably as result of thermal boundary layer re-initialization.

In this paper, a study was conducted on the heat transfer performance evaluation of two new types of pin-fin heat sinks, namely, inclined cones and wavy plate structures. The inclined cones should induce a three-dimensional motion in the flow, redirecting it towards and away from the hot plate, thereby inducing flow impingement. The wavy fins are designed to force boundary layer re-initialization and flow separation, as the flat plate fins do, while introducing a three-dimensional effect due to the curvature. The CFD methodology has been partially validated using laboratory test results and the geometry hydrodynamic and thermal performances were compared to more common geometries found in the literature. The inclined cones were then optimized using an Evolutionary Algorithm where a set of high-efficiency geometries were put forward. An important aspect of the study is the flexibility for the manufacturing of complex geometries that the newly developed surface engineering method Surfi-Sculpt® offers in comparison to classical techniques such as cold forging or machining [5, 6].

2 HYPOTHESES OF THE STUDY

This study is based on the following hypotheses: No flow bypass → the pins are attached to the top plate with adiabatic condition, surface roughness due to the manufacturing imperfections (see Fig. 1.) is neglected, gully developed flow is assumed → a periodic flow domain is chosen, 3D steady, laminar flow, incompressible fluid with constant thermodynamic properties, Prandtl number of unity since the real fluid has very high Prandtl number.

3 NUMERICAL CONFIGURATION

3.1 Governing equations

The incompressible steady 3D equations of fluid motion are solved in order to construct the flow velocity and temperature fields. The incompressibility is reflected by the constant density:

$$\rho = \text{constant} \tag{1}$$

A solenoidal velocity field:

$$\nabla \cdot U = 0 \tag{2}$$

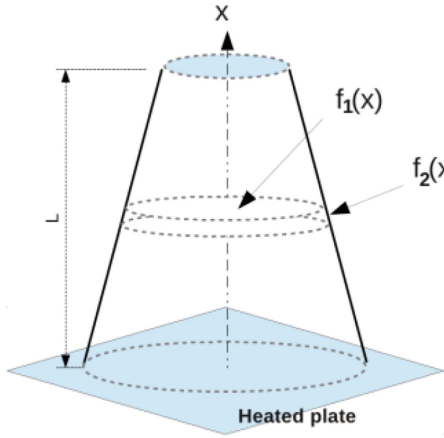

Figure 1: Inclined cone geometry for analytical thermal conduction treatment.

And the steady-state momentum equation is written as:

$$\nabla \cdot (UU) + \frac{1}{\rho}\nabla p = \nabla . \nu \ \nabla U + S_p \tag{3}$$

Where U is the velocity, p is the pressure and ν is the kinematic viscosity of the fluid. Since, in order to reduce the computational cost, a fully periodic flow is assumed, the pressure will be equal on the corresponding periodic faces. Therefore, a volumetric source term S_p is added to the momentum equation which introduces the constant pressure gradient driving the fluid to the steady-state.

The temperature equation in an incompressible flow is governed by a scalar transport-like equation which is written in steady-state as:

$$\nabla \cdot (UT) = \nabla \cdot \lambda \nabla T + S_T \tag{4}$$

Where T is the temperature and λ is the thermal diffusivity of the fluid. S_T is the driving potential for the heat transfer between the solid wall and the fluid and it is a function of the temperature gradient. The pressure compression factor and the viscous dissipation terms in the temperature transport equation are neglected due to the incompressibility and the constant thermodynamic properties of the liquid along with the unsteady term due to the flow steadiness. The thermal forcing term fixes the heat exchange and similarly the pressure forcing term is required to conform to the periodicity hypothesis.

The driving force S_p follows from the decomposition of the pressure field in a linearly varying mean pressure P and a periodic perturbation P'. Hence the pressure forcing term is defined as:

$$S_p = \frac{-1}{\rho}\frac{dP}{dx} \tag{5}$$

The driving force for the heat transfer S_T is defined similarly following from the decomposition of the temperature field in a linearly varying mean temperature T and a periodic perturbation T':

$$S_T = U\frac{dT}{dx} \tag{6}$$

It is to be noted that temperature gradient is constant imposed as input to the flow solver fixing the heat transfer rate whereas pressure gradient is adjusted in order to obtain a desired mass flow rate. Therefore, the thermal performance is characterized by the temperature difference between the hot plate and the bulk of the fluid, rather than the (imposed) value of the heat flux.

3.2 Thermal and hydrodynamic performance analysis

Due to the multitude of parameters influencing the heat transfer performance of the heat exchanger surfaces, a fair comparison is not an easy task; hence the considerable number of comparison criteria found in the literature and the variety of the results. In this study, the performance analysis was based on the method initially proposed by Colburn [7] using the pressure loss [Pa/m] against the heat transfer coefficient *h* [W/m^2.K]. The pressure loss is readily available from eqn 5 since it is iteratively calibrated to satisfy the mass flow rate. The heat transfer coefficient is computed as follows:

$$h = \frac{Q}{A_b \Delta T} \tag{7}$$

Where Q is the total heat entering into the domain, A_b is the surface of the base plate including the pin base area, rather than the wetted surface. $\Delta T = T_{inlet} - T_{wall}$ is the characteristic temperature difference between the fluid and the solid. The wall temperature T_{wall} is fixed for the computations and the fluid temperature T_{inlet} is computed by the integration of the temperature field over the periodic inlet surfaces of the domains.

3.3 Thermal conduction

Due to the low thermal conductivity ratio between the liquid and the pin material, thermal conduction through the pin should be taken into account. A rigorous approach would be the computation of the complete thermal conduction in the solid body coupled to the fluid computation in a so-called conjugate heat transfer simulation (CHT). In this work, a simpler semi-analytic approach was followed as proposed by Sahiti [8]. This was done in order to avoid the additional computational cost of a CHT treatment that would result from a long iterative process to ensure equilibrium between the CFD and the conduction solver. This would make the multi-objective optimization study, in which a large number of flow fields needs to be computed, infeasible.

The thermal conduction through the pin structures was evaluated using a differential equation for the balance between the thermal conduction through the pin base and the convection from the pin lateral surface to the working fluid. If the thermal conduction is assumed to be unidirectional along the pin axis (and, therefore, infinitely fast in other directions), this equation can be written as:

$$f_1(x)\frac{d^2T}{dx^2} + \frac{df_1(x)}{dx}\frac{dT}{dx} - \frac{h_p}{k_{pin}} f_2(x) = 0 \tag{8}$$

where $f_1(x)$ is the cross-sectional area and $f_2(x)$ is the lateral area of the pin body at a distance x from the heated plate as presented in Fig. 1. h_p is the local heat transfer coefficient of the pin as computed by the CFD simulation, assuming a uniform temperature approximation over the pin surface. k_{pin} is the thermal conductivity of the pin material. By solving the eqn (8), a temperature distribution along the pin axis was obtained. The obtained heat flux is denoted Q_{1D}, which can then be used to correct the heat flux by means of a pin efficiency, η_{pin}, defined as:

$$\eta_{pin} = \frac{Q_{1D}}{Q_{CFD}} \tag{9}$$

where $Q_{pin,max}$ is the maximum heat transferred into the liquid through the pin surface when the pin surface has the same temperature everywhere.

3.4 Computational domain, boundary and initial conditions

The flow domain is chosen to be the smallest part of the heat sink between the pins representative of the fully developed flow field in the whole pin array. The considered domain for the inclined cones is shown in Fig. 2. Four periodic surfaces of inclined cones (two are clearly present and the other two are non-present) are related in crossed manner imposing the periodicity on all the flow variables. All the other surfaces were treated as wall boundaries where the no-slip condition is applied to the momentum equation and the constant temperature applied to the temperature transport equation, except for the cold plate, which was assumed to be adiabatic.

Figure 2 also presents the flow domain between the wave structures. In this case, there are two periodic surfaces representing the inlet and the outlet of the domain, completed with six transversal surfaces grouped in two as periodic couples.

3.5 Flow solver

The steady-state incompressible momentum and temperature transport equations in 3D were solved using the simpleFoam module of the Finite Volume Solver OpenFoam. Mesh convergence was validated on the baseline geometry and the specifications were then used to generate meshes

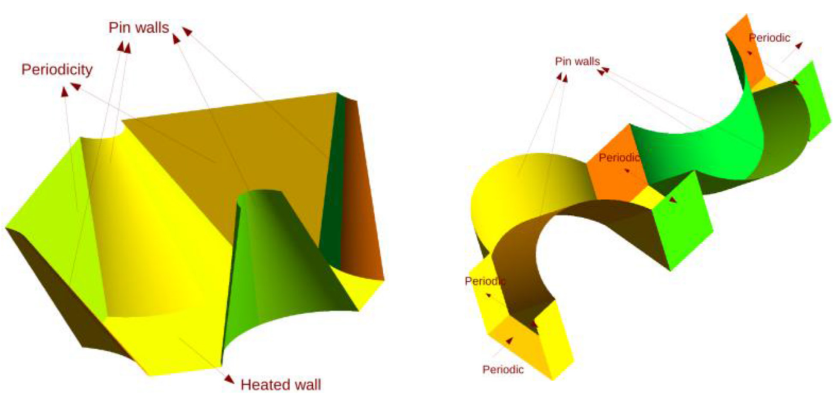

Figure 2: Numerical representation of the periodic flow domain between the inclined cone and wave structures.

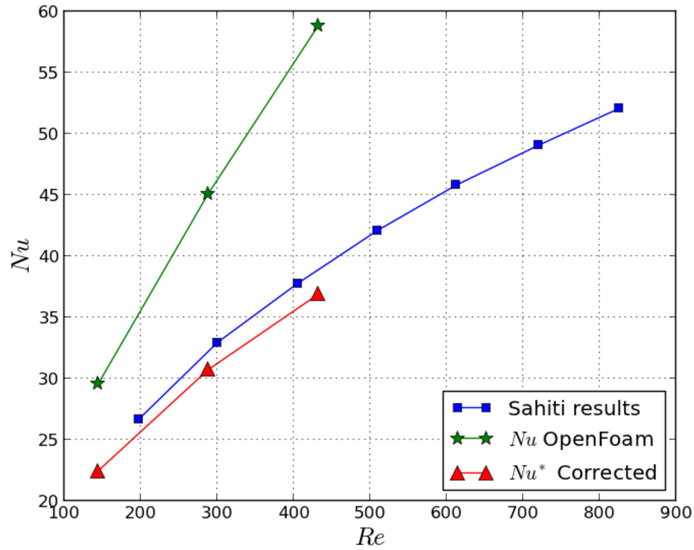

Figure 3: Comparison of the results with and without the thermal conduction (via fin efficiency) to the numerical computations of Sahiti [8].

during the optimization procedure, leading to, on average, 4×10^5 elements for each simulation. A relative iterative convergence of 10^{-4} was imposed starting from a fully uniform solution.

3.6 Validation of the thermal conduction approach

The thermal conduction approach introduced in Section 3.3 was validated against the numerical computations of Sahiti [8]. In Sahiti's work, the full CHT is treated, which should give the best approximation. Due to the limitations in this study, the simplified approach as explained in Section 3.3 was used. In Fig. 3, the application of this methodology to the results of Sahiti [8], in terms of the relationship between the Reynolds and the Nusselt numbers, is defined as:

$$Re = \frac{U_{bulk} D_h}{\nu} \quad Nu = \frac{h D_h}{k_{pin}} \tag{10}$$

Where Re is the Reynolds number, Nu is the Nusselt number, D_h is the hydraulic diameter of the pin cross-section and U_{bulk} is the volume averaged fluid velocity shown for an elliptical cross-section pin fins. The heat transfer efficiency estimated using a constant pin temperature is significantly larger than the results reported by Sahiti. However, as shown in the figure, the introduction of the fin efficiency, η_{pin}, provides a very satisfactory correction over the relevant flow regime.

4 HEAT SINK ASSESSMENT AND OPTIMIZATION

4.1 Geometry

The suggested geometries were compared to others which are currently used, including the rhombus shape. The pin profiles used in the study for comparison are rhombus, flat plate, elliptical cylinder and circular cylinder. Different variations of the proposed geometries have been tested, and include the inversion of the cones and waves (with base attached to the cold rather than to the heated plate), as well as a reduced curvature C of the waves.

The reference geometries of the standard plate and rhombus pin-fin heat sinks were specified by the industrial partner, whereas the initial baseline geometries for cylinders, cones and waves were based on a variation of geometries available in literature for the same operating conditions and global dimensions. The cone bases are represented by a major axis of (a) and a minor axis of (b). In the third dimension, the cone symmetry axis has an Φ degree inclination angle with the vertical axis. The elliptical cylinder was then generated with the same dimensions as the inclined cones at the base extruded vertically to the same height as the cones without inclination.

4.2 Validation of CFD methodology

To verify the methodology, a baseline geometry is generated for cones, curves and the rhombuses for testing. The experimental tests performed by Cooltech S.R.L are the base for the validation of the CFD methodology. Due to the confidential nature of the study, the absolute values have been excluded from the presented data.

Figure 4 presents the comparison of the pressure gradient and the heat transfer coefficient as a function of flow rate. The CFD results for the pressure drop and the heat transfer predict the experimental tendency with some discrepancy for each geometry. The discrepancy is obvious, especially in the case of the inclined cones at high fluid flow rates. The CFD increasingly underestimates the pressure drop with increasing flow rate which should be primarily due to the smooth wall assumption in numerical computations. This is verified in case of the rhombus shape fins, which are fairly smooth-walled with well-defined dimensions, the CFD results agree very well with the experimental measurements for each flow rate.

In any case, the method can be used to conduct an optimization study on the hydrodynamics where the interest is on the relative performance of geometries with respect to each other. Based on the above, the wave structures are excluded from the optimization study since their hydrodynamic performance is not promising.

In Fig. 4, the heat transfer coefficients generated by CFD analysis for three geometries are also compared to each other as well as to the experimental results. Two points are worth mentioning: the first is the systematic overestimation of the heat transfer coefficient for each case. This overestimation is common in periodic studies due to the periodicity hypothesis where the increase of the fluid temperature during its motion through the pin array is neglected. The second important point is the relative overestimation of the wave structures' thermal performance

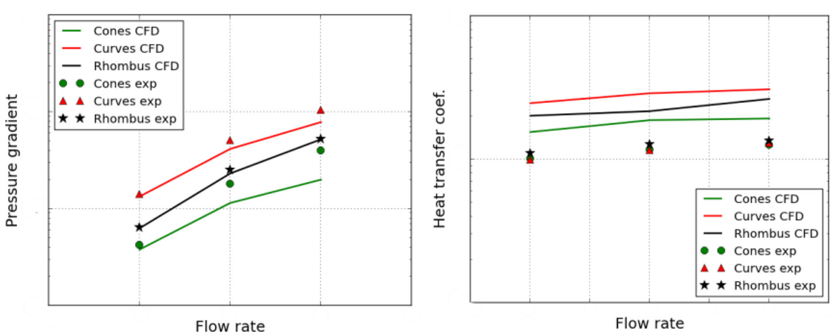

Figure 4: Comparison of the pressure drop and heat exchange coefficients through the pin array between the CFD study and the experimental measurements.

with respect to the cones and the rhombuses, which is not the case in the experimental data. Because the wave structures were excluded from the optimization study, they were not investigated any further. The relative performance between the rhombuses and the inclined cones is sufficiently well predicted as a function of the flow rate and the geometry. In this case, the neglected surface roughness is probably partially responsible for the observed discrepancies.

4.3 Comparison of baseline geometries

Figure 5 compares the thermal performances of different geometries for a given pressure drop wherein for each point presented in the figure, the mass flow rate is not the same. At a first glance, the results correspond to the results found in the literature that increasing the pressure gradient, i.e., the flow rate, helps increase the heat transfer coefficient for all geometries. A notable exception is the reference wave structure. It is also worth noting that the elliptical cylinder outperforms the circular one slightly, which also corresponds with the literature [1].

According to Fig. 5, none of the wave structures is as efficient as the rhombus structures, even though some improvements were made by modifying their geometrical configuration. From the second figure, it is evident that the inclined cones are more efficient when they are operated in the inverse mode, that is, when the heat is applied from the tip of the fin in the geometry of Fig. 2. The inverse inclined cones are thermally as efficient as the circular and the elliptical cylinders, whereas they are still behind the rhombuses for a given pressure drop. The improvement of the heat transfer efficiency in case of the inverse cones structure with respect to the original configuration is primarily related to the increase of the surface of contact on the heated plate, and not to a more favourable flow configuration (e.g. by redirection of the flow towards the heated wall) since the relative increase is slightly below the increase in the wetted area (taking into account the correction for conduction mentioned). This comparison does not indicate that the flow pattern (which is the same for the direct and inverse cones) is disadvantageous with respect to other designs.

4.4 Multi-objective optimization of inclined cone geometry

An optimization chain was created using an in-house optimization platform “Minamo” [9] in order to search for more efficient inclined cone geometries by optimizing the geometric parameters. Minamo implemented mono- and multi-objective variants of Evolutionary Algorithm strongly accelerated by the use of surrogate models, which have replaced a significant part of the costly CFD simulations. In case of a heat sink, the optimization was multi-objec-

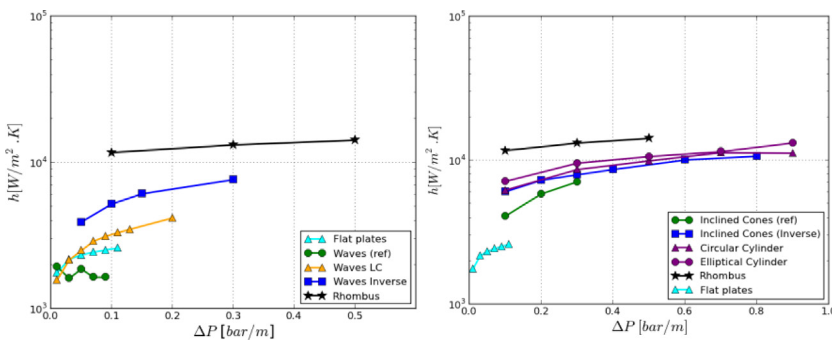

Figure 5: Comparison of different geometries in terms of thermal and hydrodynamic performance using the method of Colburn [7].

tive where the pressure drop and the heat transfer coefficient were to be optimized simultaneously. Due to the contradictory nature of these objectives, a Pareto front was constructed. None of the geometries corresponding to this front is surpassed simultaneously on both optimization targets, thereby showing the designer the compromise between the optimization targets. As a result of the observed deviations of the CFD results with respect to the experimental measurements, the optimization was only performed for the lowest flow rate where the pressure drop values agree well with the experimental measurements data for all geometries (see Fig. 4). The inclined cones have been parametrized with seven design parameters that can generate geometries with different pin dimensions, their relative positions and inclinations. Each design parameter has a minimum and a maximum value determined by the manufacturing process limitations and the geometrical restrictions from the industrial partner.

To start the optimization, Minamo requires an initial Design of Experiments (DoE) where a sufficiently large set of geometries with thermal and hydrodynamic efficiency is generated using CFD simulations. An initial DoE was created with 60 geometries (almost nine times the number of design parameters), which is typically sufficient to construct a surrogate (approximate) model. Minamo then enriches the model through an Evolutionary Algorithm by searching the DoE set and adding extra points, when necessary, validated by the CFD simulations. One hundred simulations were performed in order to enrich the surrogate model in this study in addition to the DoE set. The surrogate model quality was satisfactorily high, with a correlation coefficient of around approximately 0.94 between the predicted values and the CFD simulation results.

The Pareto efficient solutions in terms of the pressure loss and the heat transfer coefficient are shown in Fig. 6. The performances of the reference cone and the reference inverse cone along with the rhombus shape are also included in the figure for comparison. As can be seen, the optimization platform Minamo is able to identify different geometries for both the reference inclined cones and the inverse inclined cones which are advantageous, either in terms of the heat transfer or the pressure loss. The Pareto front furthermore clearly verifies the contradictory character of the objectives set for the pressure drop and the heat transfer coefficient. Inverse cones prove to be advantageous particularly in high heat transfer coefficient regions. A slight gain seems possible with respect to the rhombus shape in terms of the heat transfer efficiency, whereas the pressure loss is always lower with respect to the rhombus shapes.

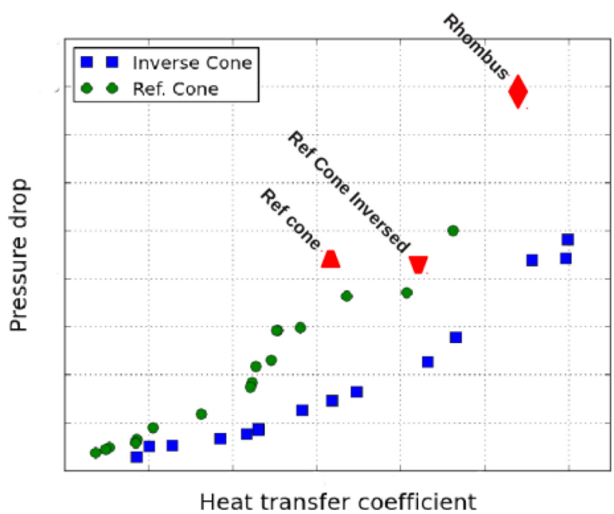

Figure 6: Pareto fronts for inverse and reference inclined cones. Each green and blue point corresponds to a different geometry.

5 CONCLUSIONS AND PROSPECTS

Two proposed heat sink geometries were analysed by means of CFD simulations in order to investigate the relative performances in comparison to the geometries found widely in the literature. The numerical analyses show that the inverse inclined cones provide a promising alternative for the efficient heat sink surfaces. Although the advantages are clear in terms of pressure drop, slightly higher thermal efficiencies than those currently obtained are also shown to be possible with inverse inclined cones. An important auxiliary consideration thereby is the strong reduction in manufacturing cost for similar performance. The next step of the work will be the experimental verification of the obtained heat transfer efficiencies and pressure drops in inverse cone's optimized versions, particularly for higher volumetric flow rates where the optimization study is much more difficult due to transitional effects. A proposition for a more robust comparison would be the optimization of the rhombus geometry by parametrizing it and comparing it to the optimized version of the inclined cones.

ACKNOWLEDGEMENTS

This project has received funding from the European Union's Seventh Framework Programme for research, technological development and demonstration under grant agreement no No 606172. The programme helps SME's outsource research increase their research efforts, extend their networks, better exploit research results and acquire technological know-how, bridging the gap between research and innovation.

REFERENCES

[1] Khan, W.A., Culham, J.R. & Yovanovich, M.M., The role of fin geometry in heat sink performance. *Journal of Electronic Packaging*, **128**, pp. 324–330, 2006. http://dx.doi.org/10.1115/1.2351896

[2] Jonsson, H. & Bjorn, P., Experimental comparison of different heat sink designs for cooling of electronics. *ASME Journal of Heat Transfer*, **329**(7), pp. 27–34, 1996.

[3] Duan, Z.Z. & Muzychka, Y.S., Pressure drop of impinge-ment air cooled plate fin heat sinks. *Journal of Electronic Packaging*, **129**, pp. 190–194, 2007. http://dx.doi.org/10.1115/1.2721094

[4] Lee, Y.J., Lee, P.S. & Chou, S.K., Enhanced thermal tran-sport in microchannel using oblique fins. *Journal of Heat Transfer*, **134**(10), 2012. http://dx.doi.org/10.1115/1.4006843

[5] Buxton, A.L., Ferhati, A., Glen, R.J.M., Dance, B.G.I., Mullen, D. & Karayiannis, T., EB surface engineering for high performance heat exchangers. *Proceeding First International Electona Beam Welding Conference*, Chicago, IL, USA, 2009.

[6] Pinto, T.M., Buxton, A.L., Neailey, K. & Barnes, S., Surface engineering improvements and opportunities with electron beams. *Eleventh International Conference on Electron Beam Technologies (EBT 2014)*, Varna, Bulgaria, 2014.

[7] Colburn, A.P., Heat transfer by natural and forced convection, Engineering Bulletin, Purdue University, Research Series, No. 84, Volume 26, pp. 47–50, 1942.

[8] Sahiti N., Thermal and fluid dynamic performance of pin fin heat transfer surfaces, Phd thesis, Erlangen University, 2006.

[9] Sainvitu, C., Ilipoulou, V. & Lepot, I., Global optimization with expensive functions – sample turbomachinery design application. *Recent Advances in Optimization and its Applications in Engineering*, Springer, pp. 499–509, 2010. http://dx.doi.org/10.1007/978-3-642-12598-0_44